Wireless 2002

THE FOURTEENTH INTERNATIONAL CONFERENCE
ON WIRELESS COMMUNICATIONS

8-10 July 2002
Coast Plaza Hotel
Calgary, Alberta
Canada

Proceedings
VOLUME 2

OFDM-CPM Signals for Indoor Wireless Communications

Imran A. Tasadduq and Raveendra K. Rao
Department of Electrical & Computer Engineering
Elborn College, 1201 Western Road
The University of Western Ontario
London, ON N6G 1H1, Canada.

Abstract—**A new class of Orthogonal Frequency Division Multiplexing - Continuous Phase Modulation (OFDM-CPM) signals has been introduced recently that out performs conventional OFDM-PSK signals. These signals employ multi-symbol observations for detection of data. An analysis of these OFDM-CPM signals has been carried out over multipath fading channels. The intent of this paper is to examine these signals for application over indoor wireless channels. Extensive simulations have been performed using industry standard SIRCIM channel simulator. Based on these results we offer design details of OFDM-CPM signals for applications in high speed indoor wireless communications.**

I. Introduction

Orthogonal Frequency Division Multiplexing (OFDM) is a wideband modulation scheme which can be designed to combat the problems of multipath propagation. In OFDM systems, the high speed data stream is converted into several parallel slower data streams with relatively longer symbol period; this will increase the system immunity to fading. Another advantage of OFDM is its high bandwidth efficiency as each of the parallel data stream's spectra overlaps with adjacent channel's spectra. The extraction of each individual channel is still possible as long as the orthogonality condition is maintained [1], [2]. Among other benefits of OFDM is that it fully exploits the advantages of digital signal processing concepts [3].

Currently, OFDM is the standard modulation scheme in Europe for Digital Audio Broadcasting (DAB) and terrestrial Digital Video Broadcasting (DVB-T). In addition, OFDM forms the basis for the physical layer in the upcoming standards for broadband WLANs, for example, European Telecommunications Standards Institute Broadband Radio Access Networks (ETSI-BRAN), Higher Performance Local Area Network (HiperLAN-2), IEEE 802.11a, Multimedia Mobile Access Communication Systems (MMAC), the fourth generation broadband wireless systems that will perform multimedia transmission to mobiles and portable PCS, for example, European MEMO project and for IEEE 802.16. [4]

This work was supported by Academic Development Fund, The University of Western Ontario under grant number R3037A02

A typical OFDM transmitter is shown in Fig. 1(a). A serial-to-parallel converter serially takes in the data stream and forms a parallel stream which is then sent to a mapper that outputs complex numbers. The mapper could be PSK, QAM, DPSK, DAPSK etc. Inverse fast Fourier transform (IFFT) is then applied to the parallel stream of complex numbers that results in orthogonal signals on the subchannels. In order to mitigate the effects of ISI, a guard interval is inserted at the transmitter and is removed at the receiver. The orthogonal signals are then converted back into a serial stream, up converted to desired carrier frequency and transmitted.

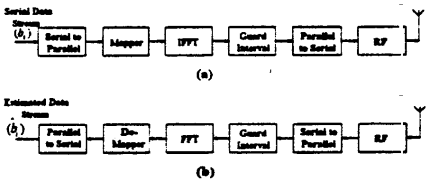

Fig. 1. OFDM transmitter and receiver

At the receiver (Fig.1(b)), the process described above is reversed. The received signal is down converted, passed through a serial-to-parallel converter, a guard interval remover, an FFT block, a de-mapper and finally a parallel-to-serial converter to eventually obtain the transmitted data sequence. In the absence of noise and fading, transmitted data is recovered without errors.

While in the literature OFDM-PSK, -QAM, -DPSK and -DAPSK have been considered, a class of OFDM-CPM signals that uses the concept of correlated phase states was recently introduced [5]. One of the advantages of these signals is that it is possible to systematically introduce correlation amongst

adjacent symbols through an appropriate choice of a parameter h[1] and permits multiple-symbol detection techniques [6]. The parameter h can be chosen to obtain a wide variety of signal mapper constellations. Furthermore, the correlation amongst OFDM symbols can be exploited in order to control bit error rate (BER). By choosing h rational and $0 < h < 1$ it is possible to have minimum number of points in the mapper constellation. An investigation of BER performance of these signals using optimum multiple-symbol detection algorithm shows that OFDM-CPM signals out perform OFDM-PSK signals over multipath fading channels. The design parameter h and the manner in which symbols are correlated give rise to a variety of signals such as single-h, multi-h, asymmetric and partial-response OFDM-CPM signals.

Since OFDM is a potential candidate for indoor wireless communications such as local area networks within buildings, it is important to evaluate its performance over measurement-based indoor wireless channels. Also, since there are numerous system and channel parameters that can affect BER in indoor mobile communications, it is extremely difficult to evaluate the performance using analytical techniques alone. Moreover, due to the complexity and time-varying nature of these indoor radio channels, it is often too complicated to design and optimize the parameters by analysis. Thus, computer simulation becomes a viable tool in performance evaluation and tradeoff analysis in the design of communication systems [7].

In this paper, we present performance of OFDM-CPM signals over realistic indoor fading channels using SIRCIM for various scenarios. In SIRCIM, a number of parameters such as carrier frequency, transmitter receiver separation, mobile speed etc. can be varied and channel impulse responses generated for these situations. We investigate the BER performance of OFDM-CPM signals by varying these parameters and highlight the configurations that achieve good performance. We also describe in detail the simulation methodology for using SIRCIM.

The paper is organized as follows. We begin with a description of OFDM-CPM signals and their properties in Section II. Next, the CPM de-mapper for detection of OFDM-CPM signals is described in Section III. In Section IV, the simulator SIRCIM is described. The channel impulse responses used in this work are described in Section V. The simulation strategy for using SIRCIM is presented in Section VI while the simulation results of OFDM-CPM signals over chosen indoor channels are presented in Section VII. The paper is concluded in Section VIII.

[1] In typical CPM signals h is modulation index

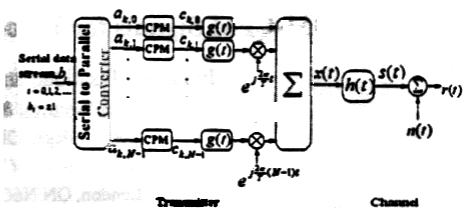

Fig. 2. OFDM-CPM Transmitter and Channel

II. OFDM-CPM Signaling Scheme

As shown in Fig. 2, serial bit stream b_i, $i = 0, 1, 2, \ldots$, with bit duration of T_b seconds is converted into blocks of N bits represented by $a_{k,p}$, $k = 0, 1, 2, \ldots$, and $p = 0, 1, 2, \ldots, N-1$, where N denotes the number of carriers and $a_{k,p} = \pm 1$. For example, $a_{0,p}$ would denote the first block of N bits and $a_{1,p}$ the second block of N bits and so on. The CPM mappers transform the incoming $a_{k,p}$ into appropriate complex numbers $c_{k,p}$ given by

$$c_{k,p} = \cos(\theta_{k,p}) + j\sin(\theta_{k,p}), \qquad (1)$$

with

$$\theta_{k,p} = a_{k,p}\pi h + \pi h \sum_{q=0}^{k-1} a_{q,p} + \phi; \qquad (2)$$

where parameter h defines the CPM mapper and ϕ represents the initial mapping point that is assumed zero without loss of generality. The angles $\theta_{k,p}$ depend not only on the current data but also on the past data. Fig. 3 shows values of $\theta_{k,p}$ as a function of time when $h = \frac{1}{2}$. Current value of θ is determined by adding $+\pi h$ (if data bit is a $+1$) or $-\pi h$ (if data bit is a -1) to the previous value of θ. The corresponding complex numbers lie on a circle.

The complex numbers from the output of CPM mappers are passed through pulse shaping filters $g(t)$, then modulated by orthogonal carriers and finally summed to give the transmitted OFDM symbol which is mathematically represented as

$$x(t) = \sum_k \sum_p c_{k,p} g(t - kT') e^{j\frac{2\pi}{T'}pt}, 0 \le t < \infty \qquad (3)$$

where

$$g(t) = \begin{cases} \frac{1}{\sqrt{T}} & -T_g \le t \le LT \\ 0 & t < -T_g, t > LT. \end{cases} \qquad (4)$$

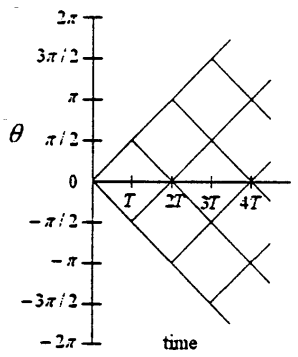

Fig. 3. Phase trellis for OFDM-CPM signaling

In Eq. (3), $T(= NT_b)$ is the OFDM symbol duration, T_g is guard interval, $T' = T_g + LT$ is the observation period and in Eq. (4) $L = 1$ for full response signaling. Throughout the analysis that follows we have assumed T_g to be sufficient to remove ISI completely.

The parameters h and L can be chosen in various ways giving rise to some of the following possible OFDM-CPM signals.

A. Single-h OFDM-CPM Signals

In this case, the value of h remains constant for all OFDM symbols. By choosing h to be rational and $0 < h < 1$ it is possible to have minimum number of points in the CPM constellation. In Fig. 4 is shown the constellation diagram of CPM mapper for $h = \frac{1}{2}$ and $h = \frac{1}{4}$.

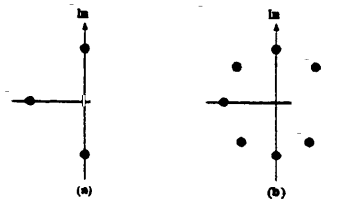

Fig. 4. Constellation diagram of CPM mapper for (a) $h = 0.5$ and (b) $h = 0.25$

B. Multi-h OFDM-CPM Signals

The value of h is cyclically chosen from a set of K values. That is, the value of h employed during the ith symbol is given by $h_l, l = i$ modulo K [8].

For example, the complex numbers of a 4-carrier OFDM-CPM signal with $H_2 = \{\frac{1}{2}, \frac{1}{4}\}$ for first two blocks of data sequences are shown below (assuming initial mapping points to be $1 + j0$):

$$[a_{k,p}, a_{k+1,p}] \implies [c_{k,p}, c_{k+1,p}],$$

$$\begin{matrix} +1 & -1 \\ +1 & +1 \\ -1 & +1 \\ +1 & -1 \end{matrix} \implies \begin{bmatrix} +j & \frac{1}{\sqrt{2}} + j\frac{1}{\sqrt{2}} \\ +j & -\frac{1}{\sqrt{2}} + j\frac{1}{\sqrt{2}} \\ -j & \frac{1}{\sqrt{2}} - j\frac{1}{\sqrt{2}} \\ +j & \frac{1}{\sqrt{2}} + j\frac{1}{\sqrt{2}} \end{bmatrix}$$

C. Asymmetric OFDM-CPM Signals

While in multi-h OFDM-CPM signals h values are independent of data bits $a_{k,p}(= \pm 1)$, in asymmetric multi-h signals h is made a function of $a_{k,p}$. That is, the value of h during the ith symbol interval is chosen h_{+i} or h_{-i} accordingly as data is a $+1$ or -1 respectively. This gives additional flexibility to the designers to optimize system performance.

D. Partial Response OFDM-CPM Signals

In Eq. (4), by making $L > 1$ the pulse duration can be extended to more than one OFDM symbol. Using a value of $L = 2, 3, \ldots$ systematic correlation can be furthered amongst OFDM symbols which in turn can be exploited for improvement in system performance.

III. Detection of OFDM-CPM Signals

A. The CPM De-mapper

A typical OFDM receiver is shown in Fig. 1(b). In this figure, the de-mapper is a decision device that decides what data most likely would have been transmitted.

Following the approach presented in [9], we design a CPM de-mapper for the recovery of transmitted data sequence. The de-mapper observes n complex numbers at the output of FFT and arrives at an optimum estimate of the data transmitted during the first bit interval. Let $\tilde{\mathbf{C}}_p$ be a vector that represents the received sequence of complex numbers at the output of FFT for pth carrier and an observation interval of n symbols. This vector is given by,

$$\tilde{\mathbf{C}}_p = [\tilde{c}_{0,p}, \tilde{c}_{1,p}, \ldots, \tilde{c}_{n-1,p}]^T$$

This vector can also be modeled as,

$$\tilde{\mathbf{C}}_p = \mathbf{C}_A + \mathbf{n} \qquad (5)$$

where $\mathbf{n} = [n_1, n_2, \ldots, n_n]^T$ represents a vector of n samples of complex Gaussian noise with a double-sided power spectral density of $\frac{N_o}{2}$. The vector $\mathbf{C}_A = [c_0, c_1, c_2, \ldots, c_{n-1}]^T$ is a sequence of complex numbers that corresponds to a transmitted data sequence $[a_0, a_1, a_2, \ldots, a_{n-1}]^T$ where $a_k = \pm 1$ and the sequence a_1 to a_{n-1} (denoted by the subscript A) represents one of the 2^{n-1} possible data sequences that would have been transmitted along with a_0. The detection problem is to observe $\tilde{\mathbf{C}}_p$ and arrive at an optimum estimate of a_0. This is a composite hypothesis testing problem stated below [10], [11].

$$\begin{aligned} H_0: &\quad \tilde{\mathbf{C}}_p = \mathbf{C}_A^{+1} + \mathbf{n} \\ H_1: &\quad \tilde{\mathbf{C}}_p = \mathbf{C}_A^{-1} + \mathbf{n}, \end{aligned} \tag{6}$$

where $\mathbf{C}_A^{+1}$ represents known sequence of complex numbers with first bit being a $+1$ and $\mathbf{C}_A^{-1}$ with first bit being a -1. The solution to this problem is the likelihood ratio test (LRT) which can be expressed as,

$$l = \frac{\int_A p\left(\tilde{\mathbf{C}}_p | H_0, A\right) p(A) dA}{\int_A p\left(\tilde{\mathbf{C}}_p | H_1, A\right) p(A) dA}, \tag{7}$$

where,

$$A = [a_1, a_2, \ldots, a_{n-1}] \tag{8}$$

$$\int_A dA = \int_{a_1}\int_{a_2}\cdots\int_{a_{n-1}} da_1 da_2 \ldots da_{n-1} \tag{9}$$

$$p(A) = p(a_1)p(a_2)\ldots p(a_{n-1}) \tag{10}$$

$$p(a_i) = \frac{1}{2}\delta(a_i - 1) + \frac{1}{2}\delta(a_i + 1). \tag{11}$$

Substituting (8)–(11) in (7), it can be shown that the likelihood ratio can be written as,

$$l = \frac{\sum_{j=1}^{m} \exp\left[\frac{1}{N_o}\mathrm{Re}\left\{\mathbf{C}_{A_j}^{+1^H}\tilde{\mathbf{C}}_p\right\}\right]}{\sum_{j=1}^{m} \exp\left[\frac{1}{N_o}\mathrm{Re}\left\{\mathbf{C}_{A_j}^{-1^H}\tilde{\mathbf{C}}_p\right\}\right]}, \tag{12}$$

where $m = 2^{n-1}$, A_j is the jth of the 2^{n-1} possible tuples of A and $\mathbf{C}^H = \mathbf{C}^{T^*}$. The corresponding receiver structure is shown in Fig. 5.

B. Recovery of Transmitted Data

After removing the guard interval, the received signal can be modeled as,

$$\left.\begin{aligned} r(t) &= x(t) * h(t) + n(t) \\ &= s(t) + n(t) \end{aligned}\right\} \quad kT' \le t \le kT' + nT,$$

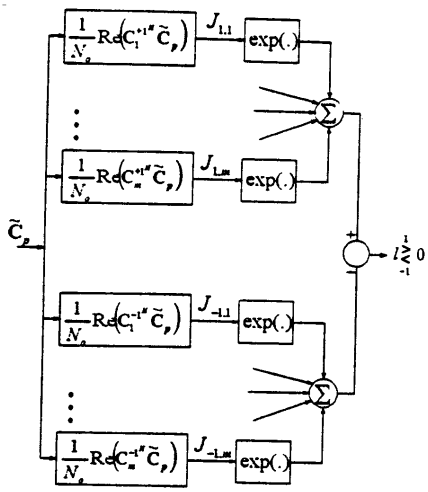

Fig. 5. CPM De-mapper

where $h(t)$ is the channel impulse response, $n(t)$ is AWGN with a double sided power spectral density of $\frac{N_o}{2}$ and * denotes convolution.

As shown in Fig. 1(b), the received signal $r(t)$ passes through several blocks before arriving at the de-mapper. For the detection of OFDM-CPM signals, this de-mapper is nothing but the receiver designed in the previous subsection. The de-mapper observes the vector $\tilde{\mathbf{C}}_p$ and arrives at an estimate of data bit a_0.

The CPM de-mapper multiplies the incoming vector $\tilde{\mathbf{C}}_p$ with all $\mathbf{C}_A^{\pm 1^H}$, takes the real part, multiplies the result with $1/N_o$, takes the exponential, adds all the resulting signals that come from $\mathbf{C}_A^{+1^H}$ and the ones that come from $\mathbf{C}_A^{-1^H}$ and takes the difference. If the difference is positive, it decides a $+1$ was transmitted else it decides in favor of a -1. For high SNR approximation of this de-mapper [9], [12], the performance can be upper bounded. This receiver at high SNR is thus given by,

$$\sum_{j=1}^{m} \exp\left(\frac{1}{N_o} J_{\pm 1,j}\right) \approx \exp\left(\frac{1}{N_o}\tilde{J}_{\pm 1}\right) \tag{13}$$

where,

$$J_{\pm 1,j} = \frac{1}{N_o}\mathrm{Re}\left\{\mathbf{C}_{A_j}^{+1^H}\tilde{\mathbf{C}}_p\right\} \tag{14}$$

and

$$\tilde{J}_{\pm 1} = \max\{J_{\pm 1,j}; j = 0, 1, \ldots, m-1\}. \quad (15)$$

Since the function exp(.) is monotonic, $\tilde{J}_{\pm 1}$ is an equivalent test parameter suggesting that the corresponding suboptimum receiver should compute all $J_{\pm 1,j}$ and produce a decision depending on the largest of these. In all our simulations we have used the high SNR approximation of the CPM de-mapper.

IV. SIRCIM Channel Simulator

SIRCIM stands for Simulation of Indoor Radio Channel Impulse response Models and it was first developed by researchers at Virginia Tech's Mobile and Portable Radio Research Group (MPRG) [13]. SIRCIM is an indoor UHF multipath radio channel software simulator that runs on a PC in conjunction with Matlab. It was designed from over 50,000 wideband and narrowband measurements from many different buildings. By providing accurate large-scale and small-scale propagation fading data, SIRCIM can be used to study bit error rates, channel access, handoff, co-channel interference, equalization, diversity, and modulation performance in frequency-flat and frequency-selective fading in building environments. SIRCIM recreates the statistics of measured wideband and narrowband impulse responses in both line of sight (LOS) and obstructed sight (OBS) topographies. LOS represent typical situations where a line of sight between transmitter and receiver exists while OBS represents situations where there is no line of sight. SIRCIM generates 19 complex impulse responses spaced $\lambda/4$ apart for a moving receiver along a 4.5λ track [14]. Statistical models for the number of multipath components, the variation of the multipath components, the amplitudes, phases and fading statistics of individual multipath components, and the excess delays are all based on measurements reported in [15]–[17].

The channel simulator also allows the user to specify the carrier frequency between 400 MHz and 60 GHz. Description of algorithms used to generate the time-varying multipath channel impulse responses are given in [18]. Additonally, the algorithm used to construct the phases of each multipath component is described in [13], [19].

Also included in SIRCIM is a continuous wave (CW) fading simulator. Wideband impulse responses over a 4.5, 10, 20, 40, or 80 wavelength track may be collapsed to generate an equivalent CW spatial fading signal over the exact same local area. In order to create the spatially varying CW fading signal, the particular wideband multipath delays and angels of arrival are used to create the spatially varying CW fading signal.

Wideband and narrowband channel impulse responses can be created in SIRCIM for open plan, hard-partitioned, and soft-partitioned buildings for LOS or OBS topographies. Details of these models are described in the following.

A. Open Plan Buildings

An open plan building environment describes buildings such as factories, warehouses and indoor sports arenas that have large open areas with a few large obstructions at irregular locations within the building. These obstructions are often large, standalone objects, such as large machines or equipment racks, which do not span from floor to ceiling [13]. SIRCIM creates wideband impulse responses in quarter wavelength increments over local areas where the complex baseband discrete impulse responses are given by

$$h_b(t, \tau_i) = \sum_{k=0}^{63} \alpha_k e^{j\theta_k} \delta(t - \tau_k) \quad (16)$$

where the power of the multipath components α_k^2, the time delays τ_k, and the phase of each multipath component θ_k are generated by SIRCIM. The angle of arrival for each multipath components is also generated and used in the computation of phase.

Many of the core models used in SIRCIM are for the case of a stationary transmitter and a mobile receiver located on the same floor within a building. In compiling the empirical database, the receiver was placed at several locations throughout different open plan buildings. At each location, the receiver was moved in a local area along a straight path called a track.

Along each 4.5λ track, multipath power delay profiles were recorded with a 7.8 ns probing pulse at 19 locations separated by $\lambda/4$. The simulator recreates power delay profiles at $\lambda/4$ separations along simulated tracks located a various transmitter-receiver (T-R) separations throughout several different open plan buildings. These tracks differ in length depending on the carrier frequency and the user's selection of the number of wavelengths per track.

B. Hard and Soft Partitioned Buildings

A typical multi-story office building with many internal partitions constructed of reinforced concrete or drywall supported by metal studs spaced 16 inches apart describes a hard partitioned building. Corridors

are typically six to ten feet wide. Walls which partition the offices from corridors are constructed from the floor to the ceiling.

Soft partitioned building describes a typical multistory office building with large open areas that are partitioned into office cubicles by 5-foot-high movable cloth covered plastic dividers.

The wideband impulse responses for soft and hard partitioned buildings are generated in the same manner as the wideband impulse responses for open plan buildings while accounting for the specific surroundings.

V. The Channel Models

Wideband impulse response of channel models used in this paper are shown in Figs. 6 and 7 for open plan building. Corresponding narrowband CW impulse responses are shown in Figs. 8 and 9. These plots show channel characteristics at the measurement location seen by a mobile user as it moves along a short track at a specified velocity. The T-R separation is assumed to be 25 m and the mobile user is assumed to be walking at a speed of 1 m/s for all simulations. The SIRCIM simulator assumes that the scatterers are aligned along aisles located to each side of the transmitter, and the width between these aisles is chosen to be 7 m for this work.

The simulator produces 19 spatially-varying complex impulse responses spaced by quarter-wavelength increments for a chosen carrier frequency which is 2600 MHz for this work. This carrier frequency implies that the length of 4.5λ track is 0.5192 m. For each complex impulse response, excess delay is 500 ns with a sampling interval of 7.8125 ns which corresponds to 64 multipaths for each of the 19 locations.

Comparing Figs. 6 and 7, it is observed that for LOS topography where there is a strong line-of-sight, most of the channel power is concentrated in the first few multipaths while for OBS topography where there is no line-of-sight, high power multipaths can be seen even after 200 ns. Corresponding narrowband CW impulse response for LOS topography in Fig. 8 shows only one strong dip in signal level that goes down to -11 dB. While the CW impulse response for OBS topography in Fig. 9 shows several such dips which go down to -19 dB.

Wideband impulse responses for LOS and OBS topographies for hard partitioned buildings are shown in Figs 10 and 11 respectively. Corresponding narrowband CW impulse responses are shown in Figs. 12 and 13. Similarly, for soft partitioned buildings, the impulse responses are shown in Figs. 14–17.

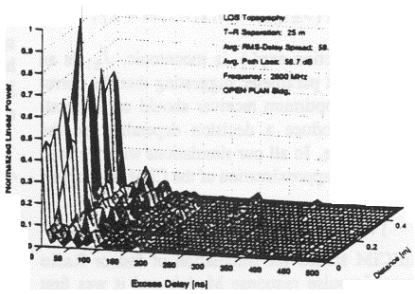

Fig. 6. Wideband impulse response for LOS channel in an open plan building

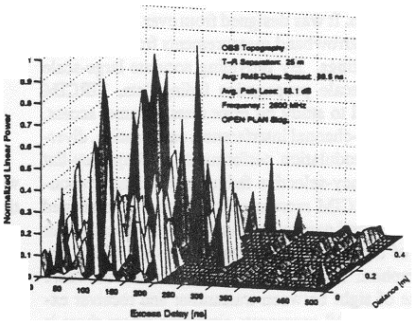

Fig. 7. Wideband impulse response for OBS channel in an open plan building

Next section describes simulation methodology that has been used to compute bit error rates using the channel models presented in this section.

VI. Simulation Methodology

A. Simulation Using Wideband Impulse Response

SIRCIM generates 19 profiles for a track length of 4.5λ. By using cubic spline interpolation on the amplitudes and phases of each multipath delay bin over space, hundreds of interpolated impulse responses between the primary profiles can be generated. The number of impulse responses to be generated using interpolation is a function of number of data symbols sent during simulation and the mobile velocity [7]. For example, if the data rate is 4 Mbps, carrier frequency 2600 MHz and mobile velocity is 1 m/s then the mobile user will take approximately 0.5 seconds

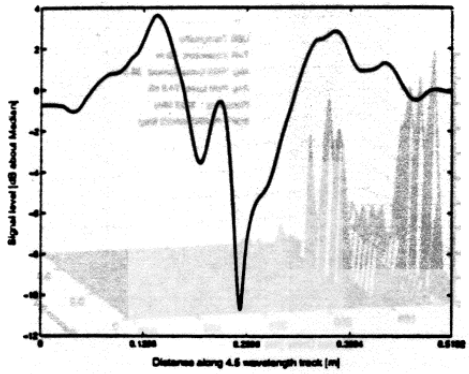

Fig. 8. Narrowband impulse response for LOS channel in an open plan building

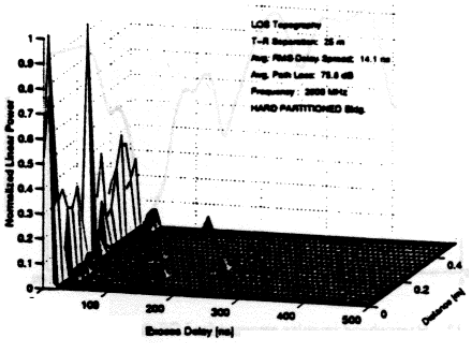

Fig. 10. Wideband impulse response for LOS channel in a hard partitioned building building

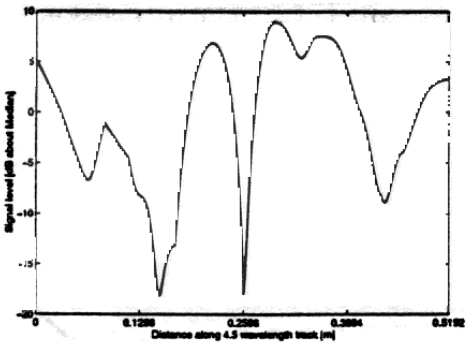

Fig. 9. Narrowband impulse response for OBS channel in an open plan building

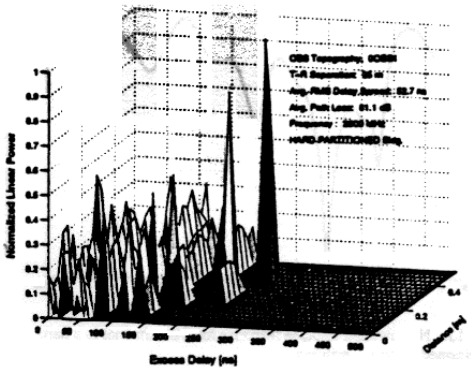

Fig. 11. Wideband impulse response for OBS channel in a hard partitioned building building

to cover a 4.5λ track. Number of data bits that will be sent during this time is 2,000,000. By assuming the channel to be stationary during the transmission of hundreds of bits (for a high data rate and slow moving receiver), number of interpolated impulse responses can be determined.

Since in most of the cases, the time delay of the channel will not match the data sampling time denoted by T_s, the time delay bins of each impulse response profile must be decimated into larger time delay bins of time period T_s to facilitate convolution. Assuming that the channel is static over T_s, all multipath components within T_s are vectorially summed to form a new multipath component. The number of multipaths are thus reduced and can be determined by dividing the maximum excess delay of the channel by the sampling period T_s.

The resulting multipath components can now be convolved with the transmitting data at each location using the following expression,

$$y(kT_s) = x(kT_s) * h_b(kT_s) \tag{17}$$

where $x(kT_s)$ is the transmitted signal sampled at kT_s, $h_b(kT_s)$ is the sampled version of channel impulse response after decimation and $y(kT_s)$ is the resultant signal after convolution.

B. Simulation Using Narrowband Impulse Response

This represents a flat fading channel where each data sample is multiplied by a complex quantity as shown below.

$$y(kT_s) = \alpha(kT_s)x(kT_s) \tag{18}$$

where α is a complex multiplicative factor [20]. Let,

$$\alpha = K\beta \tag{19}$$

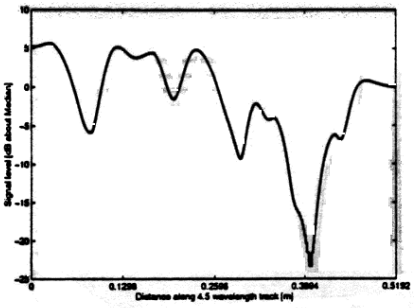

Fig. 12. Narrowband impulse response for LOS channel in a hard partitioned building building

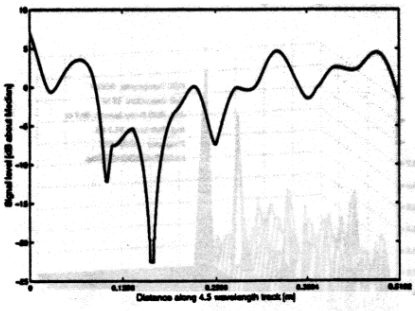

Fig. 13. Narrowband impulse response for OBS channel in a hard partitioned building building

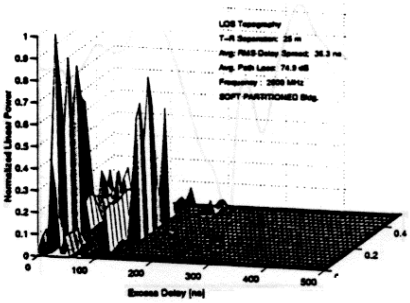

Fig. 14. Wideband impulse response for LOS channel in a soft partitioned building building

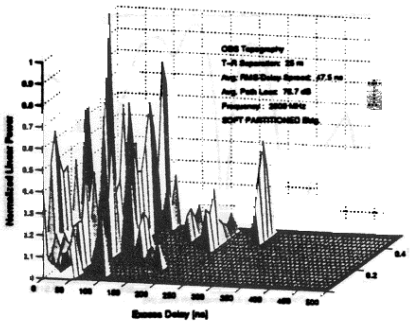

Fig. 15. Wideband impulse response for OBS channel in a soft partitioned building building

where K is a gain constant and β is a random variable with the probability distribution equal to the probability distribution of a particular CW channel used as a flat fading channel. By finding K such that

$$E\left\{|\alpha|^2\right\} = 1$$

the average energy per bit E_b in a particular simulated channel can be fixed [14].

In the case of flat fading channels, SIRCIM gives its user the option of choosing the number of interpolated profiles between each pair of $\lambda/4$ separated profiles. SIRCIM interpolates the amplitudes of fading components between consecutive profiles to simulate measurements at smaller spatial spacings and hence creates a large number of CW fading results.

VII. Numerical Results

In this section, we present BER performance of OFDM-CPM signals using the channel models described in previous sections. The parameters used for simulation are as follows. Information rate is assumed 3.2 Mbps, carrier frequency is 2600 MHz, number of carriers are 32, guard interval is 8 μs and $L = 1$ in (4). These parameters require that approximately 1,600,000 bits be sent in 0.5 seconds in order to cover the 4.5λ track.

We investigated some of the rational values of h and observed that those values of h that are closer to 0 or 1 tend to give a high BER while those in the vicinity of 0.4 and 0.6 perform better. This is to be expected because a value of $h = 4/5$ will result in constellation points that are closer to each other as compared to the ones that result for $h = 4/7$. In the latter case, it will be easier for the receiver to distinguish between adjacent signal points. Therefore, we chose some representative values of h to demonstrate the potential of OFDM-CPM signals.

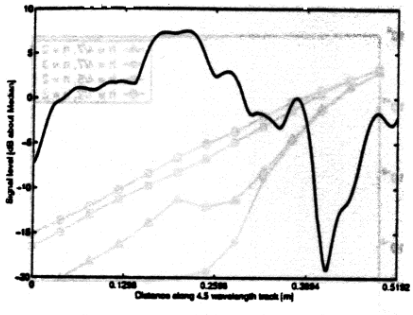

Fig. 16. Narrowband impulse response for LOS channel in a soft partitioned building building

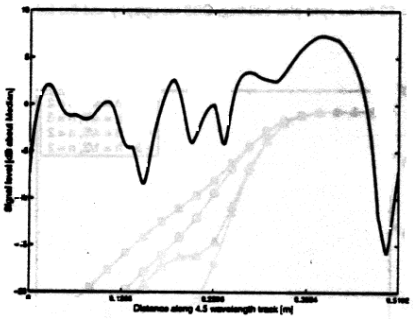

Fig. 17. Narrowband impulse response for OBS channel in a soft partitioned building building

A. Performance in Open Plan Buildings

1) Frequency-selective fading: Figure 18 shows a plot of BER versus SNR as a function of h for an OFDM-CPM system in an open plan building with line-of-sight. Impulse response of the channel used in this simulation is shown in Fig. 6. It is noted that $h = 4/7$ performs better than $h = 1/2, 4/5$ for two symbol intervals. The performance for $h = 4/7$ improves further when observation length is increased to 3. This is because the receiver now has more information to take a decision. However, we observe no appreciable improvement in performance when observation length is increased for other values of h and hence is not shown in the figure.

A plot of BER versus SNR as a function of h for an OFDM-CPM system in an open plan building is shown in Fig. 19 for an OBS topography. Corresponding channel impulse response is shown in Fig. 7. Since there is no line-of-sight, system performance is inferior to what was shown in Fig. 18. However, $h = 4/7$ with an observation length of 3 symbols out performs $h = 1/2, 4/5$ and $h = 4/7$ with $n = 2$.

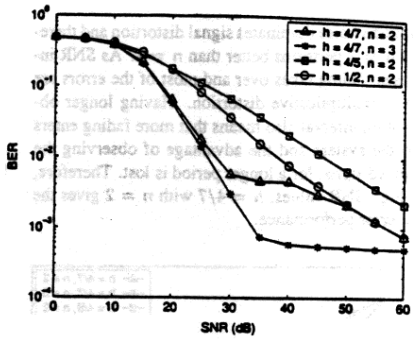

Fig. 18. BER as a function of SNR for various values of h with $N = 32$ for an open plan building and LOS topography

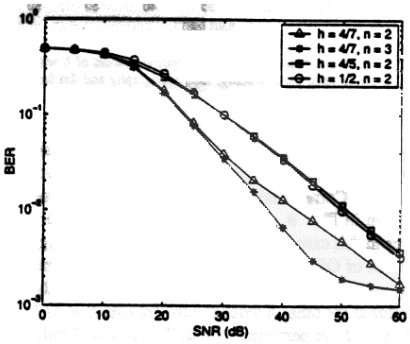

Fig. 19. BER as a function of SNR for various values of h with $N = 32$ for an open plan building and OBS topography

2) Flat fading: Figure 20 shows a plot of BER versus SNR as a function of h for an OFDM-CPM system in an open plan building with line-of-sight. Impulse response of the channel used in this simulation is shown in Fig. 8. It is noted that $h = 4/7$ performs better than $h = 1/2, 4/5$ for two symbol intervals. The performance for $h = 4/7$ improves further when observation length is increased to 3. However, for SNR values greater than 45 dB, $h = 4/7$ with an observation length of 2 symbols out performs $h = 4/7$ with $n = 3$. Such a behavior is observed due to the fact that for low SNR values,

Gaussian noise dominates signal distortion and therefore $n = 3$ performs better than $n = 2$. As SNR increases, fading takes over and most of the errors are due to multiplicative distortion. Having longer observation interval also means that more fading enters into the system and the advantage of observing the received signal for a longer period is lost. Therefore, for high SNR values, $h = 4/7$ with $n = 2$ gives the best error performance.

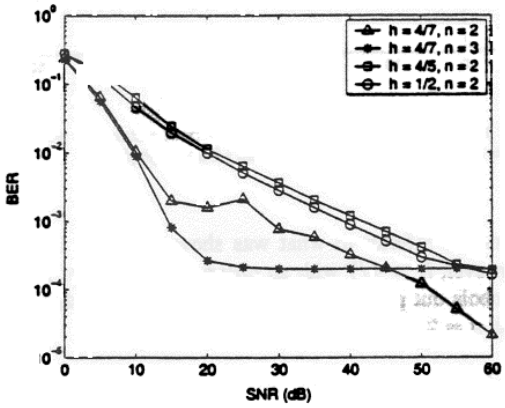

Fig. 20. BER as a function of SNR for various values of h with $N = 32$ for an open plan building, LOS topography and flat fading

BER performance of an OFDM-CPM system in an open plan building without a line-of-sight is shown in Fig. 21. Corresponding channel impulse response is shown in Fig. 9. Although, overall BER performance in this case is inferior to the one shown in Fig. 20, BER of OFDM-CPM system with $h = 4/7$ and an observation interval of 3 symbols is substantially superior to the other h values. Furthermore, $h = 4/7$ with $n = 2$ out performs $h = 4/7$ with $n = 3$ only beyond 55 dB SNR.

B. *Performance in Hard Partitioned Buildings*

1) Frequency-selective fading: Figure 22 shows a plot of BER versus SNR as a function of h for an OFDM-CPM system in a hard partitioned building with line-of-sight. Impulse response of the channel used in this simulation is shown in Fig. 10. It is noted that the overall BER performance is inferior to that of open plan building and $h = 4/7$ with an observation length of 3 symbols achieves the best BER performance.

A plot of BER versus SNR as a function of h for an OFDM-CPM system in a hard partitioned building is shown in Fig. 23 for an OBS topography. Corresponding channel impulse response is shown in

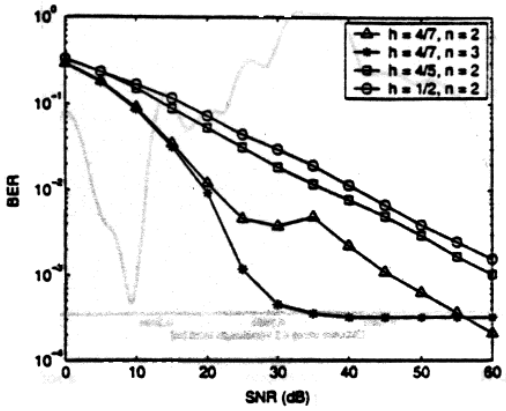

Fig. 21. BER as a function of SNR for various values of h with $N = 32$ for an open plan building, OBS topography and flat fading

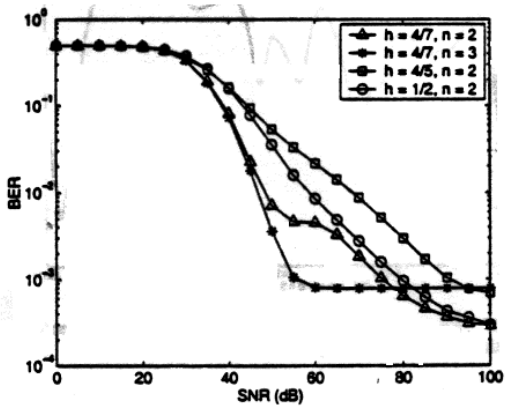

Fig. 22. BER as a function of SNR for various values of h with $N = 32$ for a hard partitioned building and LOS topography

Fig. 11. Since there is no line-of-sight, system performance is inferior to what was shown in Fig. 22. However, $h = 4/7$ with an observation length of 3 symbols out performs $h = 1/2, 4/5$ and $h = 4/7$ with $n = 2$. Furthermore, $h = 4/5$ and $h = 1/2$ achieve nearly the same BER performance. It is observed that beyond 70 dB SNR, performance of $h = 1/2, 4/5$ and $h = 4/7$ is nearly the same for an observation length of 2 symbols.

2) Flat fading: Figure 24 shows a plot of BER versus SNR as a function of h for an OFDM-CPM system in a hard partitioned building with line-of-sight. Impulse response of the channel used in this simulation is shown in Fig. 12. It is noted that for SNR greater than 55 dB, $h = 4/7$ with $n = 2$ out performs $h = 4/7$ and $n = 3$. For SNR values be-

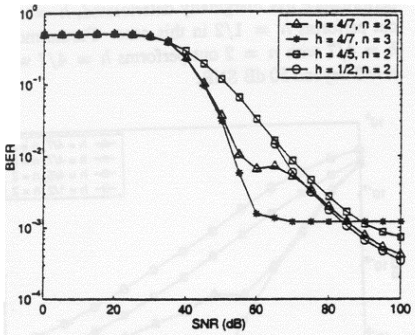

Fig. 23. BER as a function of SNR for various values of h with $N = 32$ for a hard partitioned building and OBS topography

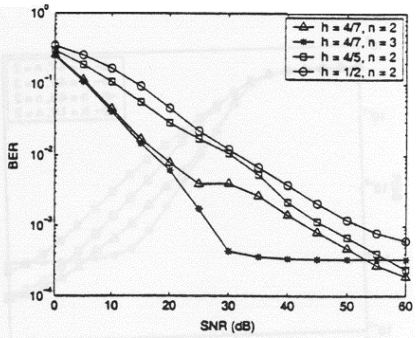

Fig. 25. BER as a function of SNR for various values of h with $N = 32$ for a hard partitioned building, OBS topography and flat fading

tween 30 dB and 50 dB, an OFDM-CPM system with $h = 4/7$ and $n = 3$ achieves the best BER performance.

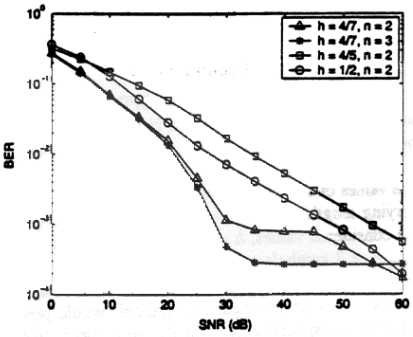

Fig. 24. BER as a function of SNR for various values of h with $N = 32$ for a hard partitioned building, LOS topography and flat fading

BER performance of an OFDM-CPM system in a hard partitioned building without a line-of-sight is shown in Fig. 25. Corresponding channel impulse response is shown in Fig. 13. It is noted that $h = 4/7$ with $n = 3$ achieves almost the same performance as was observed for the case of line-of-sight. Furthermore, the performance of $h = 4/7$ and $h = 1/2$ with $n = 2$ has deteriorated especially for SNR values between 30 dB and 50 dB.

C. Performance in Soft Partitioned Buildings

1) Frequency-selective fading: BER performance of an OFDM-CPM system in a soft partitioned building with line-of-sight is shown in Fig. 26. Corresponding channel impulse response is shown in Fig. 14. It is observed that the BER performance of the system is similar to the performance in a hard partitioned building. In this case, $h = 4/7$ with $n = 3$ achieves the best BER performance until around 80 dB SNR. Moreover, $h = 1/2$ and $h = 4/7$ with an observation interval of 2 symbols achieve nearly the same performance beyond an SNR of 80 dB.

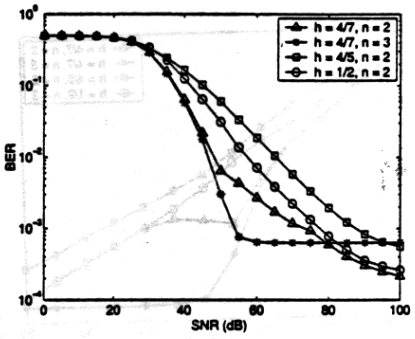

Fig. 26. BER as a function of SNR for various values of h with $N = 32$ for a soft partitioned building and LOS topography

Figure 27 shows a plot of BER versus SNR as a function of h for an OFDM-CPM system in a soft partitioned building without line-of-sight. Impulse response of the channel used in this simulation is shown in Fig. 15. Since there is no line-of-sight, system performance is inferior to what was shown in

Fig. 26. Also, $h = 4/7$ with an observation length of 3 symbols is marginally superior to $h = 1/2, 4/5$ and $h = 4/7$ with $n = 2$.

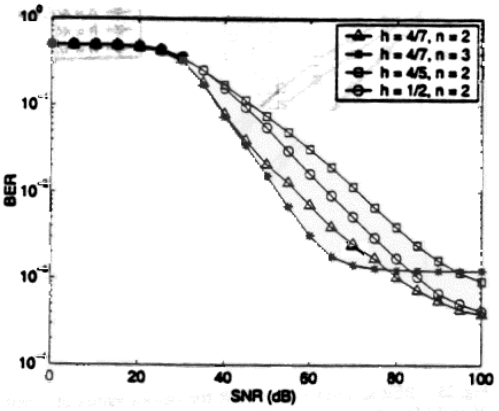

Fig. 27. BER as a function of SNR for various values of h with $N = 32$ for a soft partitioned building and OBS topography

2) Flat fading: Figure 28 shows a plot of BER versus SNR as a function of h for an OFDM-CPM system in a soft partitioned building with line-of-sight. Impulse response of the channel used in this simulation is shown in Fig. 16. It is noted that the BER performance of $h = 4/7$ with $n = 3$ is far superior to other h values considered. Moreover, for an observation length of 2 symbols, the performance of $h = 4/7$ and $h = 1/2$ becomes nearly the same for SNR values greater than 40 dB.

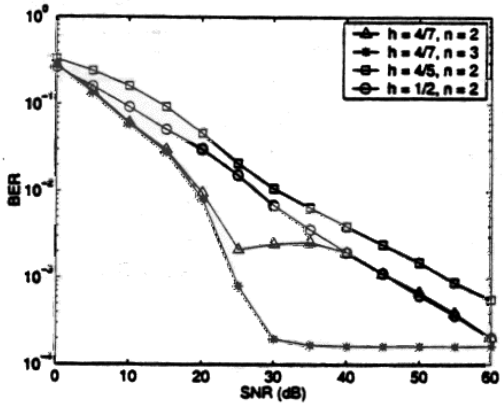

Fig. 28. BER as a function of SNR for various values of h with $N = 32$ for a soft partitioned building, LOS topography and flat fading

BER performance of an OFDM-CPM system in a soft partitioned building without a line-of-sight is shown in Fig. 29. Corresponding channel impulse response is shown in Fig. 17. Although, overall BER performance has marginally deteriorated, $h = 4/5$ out performs $h = 1/2$ in this case. Furthermore, $h = 4/7$ with $n = 2$ out performs $h = 4/7$ with $n = 3$ beyond 50 dB SNR.

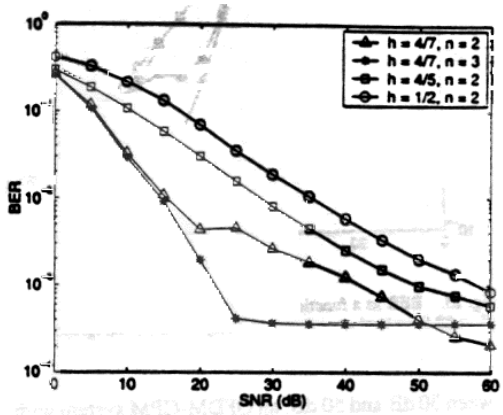

Fig. 29. BER as a function of SNR for various values of h with $N = 32$ for a soft partitioned building, OBS topography and flat fading

VIII. Conclusions

BER performance of uncoded OFDM-CPM signals was presented over mobile indoor radio channels. It was shown that OFDM-CPM is a promising signaling scheme for indoor fading channels. Various values of the design parameter h were used with varying lengths of observation intervals. Amongst the considered values, $h = 4/7$ with an observation length of 3 symbols achieved the best BER performance. However, for very high SNR values, $h = 4/7$ with an observation length of 2 symbols would perform better; especially for open plan buildings and/or flat fading channels. It was also observed that $h = 1/2$ performs better for topographies where there is a strong line-of-sight rather than those where there is no line-of-sight.

Computation of optimum values of h and observation interval n that would optimize BER performance of an OFDM-CPM system remains to be investigated. This would require development of analytical expressions for BER and application of some optimization algorithms in order to find optimum or suboptimum values of h and n that would give minimum error rate.

In order to reduce receiver complexity, Viterbi decoders can be employed for detection of OFDM-CPM signals. This can be easily implemented when

h is chosen as the ratio of two integers, p and q. Then the Viterbi decoder has to keep track of either q states if p is even or $2q$ states if p is odd.

ACKNOWLEDGEMENTS

We thank Dr. Theodore S. Rappaport of Virginia Polytechnic Institute for helpful discussions regarding the use of SIRCIM simulator.

REFERENCES

[1] J.A.C. Bingham, "Multicarrier modulation for data transmission: An idea whose time has come," *IEEE Communications Magazine*, pp. 5–14, May 1990.

[2] Leonard J. Cimini Jr., "Analysis and simulation of a digital mobile channel using orthogonal frequency division multiplexing," *IEEE Trans. on Comm.*, vol. 33, no. 7, pp. 665–675, July 1985.

[3] S.B. Weinstein and Paul M. Ebert, "Data transmission by frequency-division multiplexing using the discrete Fourier transform," *IEEE Trans. on Comm. Tech.*, vol. 19, no. 5, pp. 628–634, October 1971.

[4] Andreas F. Molisch, *Wideband Wireless Digital Communications*, Prentice Hall PTR, 2001.

[5] Imran A. Tasadduq and Raveendra K. Rao, "OFDM-CPM signals," *Electronics Letters*, vol. 38, no. 2, pp. 80–81, 17 January 2002.

[6] Imran A. Tasadduq and Raveendra K. Rao, "Detection of OFDM-CPM signals over multipath channels," *IEEE International Conference on Communications, ICC'2002*, 28 April-02 May 2002.

[7] Victor Fung and Theodore S. Rappaport, "Bit error simulation for $\pi/4$ DQPSK mobile radio communications using two-ray and measurement-based impluse response models," *IEEE Journal on Selected Areas in Comm.*, vol. 11, no. 3, pp. 393–405, April 1993.

[8] John B. Anderson and Desmond P. Taylor, "A bandwidth-efficient class of signal-space codes," *IEEE Transactions on Information Theory*, vol. 24, no. 6, pp. 703–712, November 1978.

[9] William P. Osborne and Michael B. Luntz, "Coherent and noncoherent detection of CPFSK," *IEEE Trans. on Comm.*, vol. 22, no. 8, pp. 1023–1036, August 1974.

[10] Robert N. McDonough and Anthony D. Whalen, *Detection of Signals in Noise*, San Diego: Academic Press, 1995.

[11] H.L. Van Trees, *Detection, Estimation and Modulation Theory, Part I*, New York: Wiley, 1968.

[12] Walter Hirt and Subbarayan Pasupathy, "Continuous phase chirp (CPC) signals for binary data communication - part I: coherent detection," *IEEE Transactions on Communications*, vol. 29, no. 6, pp. 836–847, June 1981.

[13] Wireless Valley Communications, Inc., *SIRCIM 6.0 User's Manual*, January 2001.

[14] Victor Fung, "Bit error simulation of FSK, BPSK, and $\pi/4$ DQPSK in flat and frequency-selective fading mobile radio channels using two-ray and measurement-based impulse response models," Master's thesis, Virginia Polytechnic Institute and State University, August 1991.

[15] Theodore S. Rappaport, Scott Y. Seidel, and Koichiro Takamizawa, "Statistical channel impulse response models for factory and open plan building radio communication system design," *IEEE Transactions on Communications*, vol. 39, no. 5, pp. 794–807, May 1991.

[16] Theodore S. Rappaport and Clare D. McGillem, "UHF fading in factories," *IEEE Journal on Selected Areas in Communications*, vol. 7, no. 1, pp. 40–48, January 1989.

[17] Theodore S. Rappaport, "Characterization of UHF multipath radio channels in factory buildings," *IEEE Transactions on Antennas and Propagation*, vol. 37, no. 8, pp. 1058–1069, August 1989.

[18] S.Y. Seidel and T.S. Rappaport, "Simulation of UHF indoor radio channels for open plan building environments," *40th IEEE Vehicular Technology Conference, Orlando, FL*, pp. 597–602, May 1990.

[19] D.M. Krizman, B.J. Ellison, and T.S. Rappaport, "Modeling and simulation of narrowband phase from wideband channel impulse response," *IEEE Vehicular Technology Conference*, pp. 67–71, 1997.

[20] Theodore S. Rappaport and Victor Fung, "Simulation of bit error performance of FSK, BPSK, and $\pi/4$ DQPSK in flat fading indoor radio channels using a measurement-based channel model," *IEEE Tran. on Veh. Tech.*, vol. 40, no. 4, pp. 731–740, November 1991.